

Published in final edited form as:

Science. 2013 January 11; 339(6116): . doi:10.1126/science.1227568.

JNK Expression by Macrophages Promotes Obesity-induced Insulin Resistance and Inflammation

Myoung Sook Han^{1,2}, Dae Young Jung², Caroline Morel^{1,2}, Saquib A. Lakhani^{4,†}, Jason K. Kim^{2,3}, Richard A. Flavell⁴, and Roger J. Davis^{1,2,*}

¹Howard Hughes Medical Institute, Worcester, Massachusetts 01605, USA

²Program in Molecular Medicine and the University of Massachusetts Medical School, Worcester, Massachusetts 01605, USA

³Department of Medicine, Division of Endocrinology, Metabolism and Diabetes, University of Massachusetts Medical School, Worcester, Massachusetts 01605, USA

⁴Howard Hughes Medical Institute and Department of Immunobiology, Yale University School of Medicine, New Haven, Connecticut 06520, USA

Abstract

The cJun NH₂-terminal kinase (JNK) signaling pathway contributes to inflammation and plays a key role in the metabolic response to obesity, including insulin resistance. Macrophages are implicated in this process. To test the role of JNK, we established mice with selective JNK-deficiency in macrophages. We report that feeding a high fat diet to control and JNK-deficient mice caused similar obesity, but only mice with JNK-deficient macrophages remained insulin sensitive. The protection of mice with macrophage-specific JNK-deficiency against insulin resistance was associated with reduced tissue infiltration by macrophages. Immunophenotyping demonstrated that JNK was required for pro-inflammatory macrophage polarization. These studies demonstrate that JNK in macrophages is required for the establishment of obesity-induced insulin resistance and inflammation.

Obesity is an important public health problem that is associated with inflammation, cardiovascular disease, metabolic syndrome, and type 2 diabetes (1). Tissue infiltration by macrophages is a major contributor to inflammation and insulin resistance (2). Tissue macrophages comprise multiple populations (3); however, there are two well known subtypes that are capable of dynamic inter-conversion (4). Classically activated macrophages (M1) induced by interferon (IFN)- or endotoxin promote interleukin (IL)-12-mediated T helper 1 (Th1) immune responses. Alternatively activated macrophages induced by IL4 or IL13 (M2a), immune complexes (M2b), and the anti-inflammatory cytokines IL10 or transforming growth factor- (M2c) can promote Th2 immune responses and mediate wound healing, tissue repair, and the resolution of inflammation. Obesity increases tissue infiltration by macrophages (5) and polarization to the pro-inflammatory M1 state (6, 7) (fig. S1). Indeed, the inflammation associated with M1 polarized tissue macrophages is implicated in the development of obesity-related insulin resistance (8–11).

Signal transduction pathways in macrophages that are responsive to obesity represent possible targets for therapeutic intervention in obese patients. One example is the stress-responsive cJun NH₂-terminal kinase (JNK) signal transduction pathway that is activated by

*Correspondence to: Roger.Davis@umassmed.edu.

†Present Address: Department of Pediatrics, Sanford University School of Medicine, Sioux Falls, SD 57117, USA

obesity and is required for obesity-induced insulin resistance (12). Two genes (*Jnk1* and *Jnk2*) encode JNK proteins in peripheral insulin-responsive tissues. JNK1 plays a critical role in adipose tissue and muscle (but not liver) during the development of insulin resistance (12). JNK1 in the hypothalamus is also required for high fat diet (HFD)-induced obesity (12). Whether JNK plays a role in macrophages is unclear, with evidence both for and against having been reported (13–15). For instance, JNK1-specific deficiency in macrophages (14) and JNK2-deficiency (16) causes no defect in obesity-induced insulin resistance, which suggests that JNK expression in macrophages may play no role. Alternatively, JNK1 and JNK2 may function redundantly. Studies of the effect of compound deficiency of JNK1 plus JNK2 in macrophages are required to distinguish between these possibilities.

To test the role of macrophage JNK, we established control (*Lyz2-Cre⁺Jnk1^{+/+}Jnk2^{+/+}*) mice and mice with a macrophage-specific ablation of JNK (*Lyz2-Cre⁺Jnk1^{LoxP/LoxP}Jnk2^{LoxP/LoxP}*) (fig. S2). Genotype analysis demonstrated specific disruption of the *Jnk1* and *Jnk2* genes in macrophages isolated from JNK-deficient (KO) mice, but not control (WT) mice (fig. S2). This conclusion was confirmed by immunoblot analysis of JNK expression in macrophages isolated from WT and KO mice (fig. S3A). Impaired phosphorylation of the canonical JNK substrate cJun (17) in KO macrophages confirmed that JNK signaling was disrupted in these cells (fig. S3B,C).

Comparison of WT and KO mice demonstrated that these animals exhibited similar obesity when fed a HFD, although a slight reduction in lean mass was detected in KO mice compared with WT mice fed a normal chow diet (fig. S4). Chow-fed WT and KO mice displayed similar insulin and glucose tolerance, and blood concentrations of glucose and insulin (Fig. 1A–E). Feeding a HFD to WT mice caused hyperglycemia, hyperinsulinemia, and intolerance to both glucose and insulin (Fig. 1A–E). In contrast, KO mice were protected against these effects of a HFD. Specifically, macrophage-specific JNK-deficiency prevented HFD-induced hyperglycemia and hyperinsulinemia, and also improved both insulin and glucose tolerance compared with HFD-fed WT mice (Fig. 1A–E). In contrast, the blood concentration of glycerol and free fatty acids in HFD-fed WT and KO mice was similar (fig. S5), suggesting that macrophage-specific JNK-deficiency may not prevent obesity-associated lipolysis. Together, these data demonstrate similar diet-induced obesity phenotypes of WT and KO mice; however, the HFD-fed KO mice remained insulin sensitive compared with HFD-fed WT mice.

We performed hyperinsulinemic-euglycemic clamp studies to directly assess insulin sensitivity of WT and KO mice *in vivo* (Fig. 1F–J). This analysis demonstrated that KO mice exhibited increased whole body insulin sensitivity because of significant improvements in glucose infusion rates during the clamps (Fig. 1F), hepatic insulin action (Fig. 1G), hepatic glucose production (Fig. 1H), insulin-stimulated whole body glucose turnover (Fig. 1I), and whole body glycogen plus lipid synthesis (Fig. 1J) compared with WT mice. We also performed biochemical studies to investigate insulin-stimulated AKT activation in WT and KO mice (Fig. 1K). Feeding a HFD suppressed insulin-stimulated AKT activation in liver, adipose tissue, and muscle of WT mice but not KO mice (Fig. 1K). Together, these data demonstrate that HFD-fed KO mice exhibit improved insulin sensitivity compared with HFD-fed WT mice.

Pancreatic islets in chow-fed WT and KO mice were morphologically similar. Feeding a HFD to WT mice, but not KO mice, caused cell proliferation, islet hypertrophy, and suppression of glucose-stimulated insulin secretion *in vivo* and *in vitro* (Fig. 2A–F). These data are consistent with the observation that HFD-fed KO mice exhibit improved

hyperglycemia, hyperinsulinemia, and insulin sensitivity compared with HFD-fed ^{WT} mice.

We examined adipose tissue macrophages (ATM) in ^{WT} and ^{KO} mice fed a chow or a HFD. No differences in the number of ATM were detected in ^{WT} and ^{KO} mice fed a chow diet, whereas feeding a HFD caused an increase in the number of ATM in ^{WT} mice, but not ^{KO} mice (Figs. 3A, S4, S6). These data indicate that JNK in macrophages promotes HFD-induced accumulation of ATM. In contrast, we observed no significant differences in the number of infiltrating eosinophils or neutrophils (figs. S7, S8).

M1 polarized tissue macrophages are implicated in the development of insulin resistance (6–10). We therefore performed immunophenotyping to examine the populations of ATM in ^{WT} and ^{KO} mice. Macrophage-specific JNK-deficiency prevented the accumulation of ATM expressing surface markers (F4/80⁺ CD11c⁺ CD206⁻) associated with M1 polarization in adipose tissue of HFD-fed mice (Figs. 3B, S6). In contrast, no significant difference in the accumulation of ATM expressing surface markers (F4/80⁺ CD11c⁻ CD206⁺) associated with M2 polarization between HFD-fed ^{WT} and ^{KO} mice was detected (Figs. 3C, S6). These data indicate that JNK expression by macrophages promotes the accumulation of M1 polarized ATM in HFD-fed mice.

To confirm whether JNK influences the accumulation and polarization of ATM, we examined adipose tissue gene expression (Fig. 3D). This analysis demonstrated that macrophage-specific JNK-deficiency decreased the expression of ATM marker genes (*Cd68*, *F4/80*) in adipose tissue of HFD-fed ^{KO} mice compared with HFD-fed ^{WT} mice. Moreover, gene expression associated with M1 polarization (*Cd11c*, *Il1*, *Il6*, *Nos2*, *Tnf*) and M2 polarization (*Arg1*, *Il10*, *Mgl1* (*Cd301*), *Mgl2*, *Mrc1* (*Cd206*), *Mrc2*) demonstrated that macrophage-specific JNK-deficiency decreased the expression of genes associated with M1 polarization and increased those associated with M2 polarization in ATM in HFD-fed mice (Fig. 3D). These data confirm that JNK expression in macrophages promotes both ATM accumulation and M1 polarization in HFD-fed mice.

To further test the role of JNK in the polarization of tissue macrophages, we examined the liver of ^{WT} and ^{KO} mice (fig. S9). Macrophage-specific JNK-deficiency resulted in a decrease in the hepatic expression of tissue macrophage marker genes and genes associated with M1 polarization, whereas expression of genes associated with M2 polarization were increased in HFD-fed ^{KO} mice compared with HFD-fed ^{WT} mice (fig. S9C). These data demonstrate that JNK expression by macrophages is required for tissue macrophage accumulation in the liver and polarization to the activated M1 state in HFD-fed mice. The decreased accumulation of M1 tissue macrophages in the liver of HFD-fed ^{KO} mice was associated with a marked reduction in hepatic inflammation and gluconeogenesis compared with HFD-fed ^{WT} mice (figs. S9C,D).

The chemokine signaling network is implicated in tissue macrophage function (18). Mice deficient in the chemokine receptors CCR2 or CCR5 have defects in HFD-induced ATM accumulation (7, 19). Immunophenotyping suggests preferential loss of M1 ATM in *Ccr5*^{-/-} mice (19) and M2 ATM in *Ccr2*^{-/-} mice (7). Expression of CCR2 ligands (CCL2, CCL7, CCL8) and CCR5 ligands (CCL3, CCL4, CCL5, CCL8) was increased when ^{WT} mice were fed a HFD (figs. S10A, S11, S12). In contrast, HFD-induced chemokine expression was largely suppressed in HFD-fed ^{KO} mice (figs. S10A, S11, S12). Moreover, JNK-deficiency reduced chemokine expression by macrophages *in vitro* under a variety of stimulation conditions (figs. S10B, S13, S14, S15). Because tissue chemokine expression is mediated by both parenchymal cells and macrophages, it is likely that the reduced chemokine expression detected in HFD-fed ^{KO} mice is a consequence of both a primary

macrophage defect and a secondary response to improved glycemia. Collectively, these data indicate that reduced chemokine signaling may contribute to the decreased accumulation of ATM in ^{KO} mice. However, no selective defect in the expression of CCR2 or CCR5 receptors or ligands was detected in ^{KO} mice compared with ^{WT} mice. The loss of M1 ATM in ^{KO} mice may therefore represent an intrinsic defect in M1 polarization rather than inefficient M1 ATM recruitment.

To test the requirement of JNK for M1 macrophage function *in vitro*, we isolated bone marrow-derived macrophages (BMDM) from ^{WT} and ^{KO} mice (Fig. 4). Treatment with IFN- γ causes M1 differentiation (3) and expression of the cell surface marker CD11c (20). Macrophage-specific JNK-deficiency caused reduced M1 differentiation compared to control mice (Fig. 4A). Furthermore, JNK-deficiency caused decreased expression of M1 marker genes (*Ccr7*, *Cd11c*), chemokines (*Ccl2*, *Ccl5*), and cytokine genes (*Il1*, *Il6*, *Il12*, *Tnf*) in IFN- γ stimulated macrophages (Figs. 4B, S14). Similar defects were detected in lipopolysaccharide (LPS)-stimulated macrophages (fig. S15). Moreover, the blood concentration of M1-associated cytokines and chemokines was significantly reduced in LPS-treated ^{KO} mice compared with ^{WT} mice *in vivo* (Fig. 4C). Together, these data demonstrate that JNK-deficiency suppresses M1 polarization. In contrast, no significant difference in M2 differentiation between BMDM isolated from ^{WT} and ^{KO} mice was detected (figs. S16, S17, S18).

The observation that JNK is required for the differentiation of pro-inflammatory macrophages provides an explanation, in part, for previous findings that have implicated JNK in inflammatory responses (17), including the promotion of Th1 immune responses (21–23). JNK-dependent inflammatory macrophages in the liver may account for the requirement of JNK for the development of fulminant hepatitis in mouse models (24). JNK-dependent tissue macrophages may also contribute to the inflammation associated with insulin resistance caused by obesity. Indeed, JNK in macrophages is required for the accumulation of inflammatory tissue macrophages and insulin resistance caused by diet-induced obesity. Drug-mediated targeting of macrophage-expressed JNK therefore represents a potential therapeutic approach to suppress inflammation that may be applicable to the treatment of inflammatory disorders.

Supplementary Material

Refer to Web version on PubMed Central for supplementary material.

Acknowledgments

We thank T. Barrett, V. Benoit, Y. Lee, and J-H. Liu for technical assistance, S. Vernia for designing Taqman probes, and K. Gemme for administrative assistance. These studies were supported by grants from the National Institutes of Health (DK090963, DK080756, and CA065861). The UMASS Mouse Metabolic Phenotyping Center is supported by grant DK093000. M.S.H. was supported by a post-doctoral fellowship (7-10-BETA-02) from the American Diabetes Association. R.J.D. and J.K.K. are members of the UMASS Diabetes and Endocrinology Research Center (DK032520). R.J.D. and R.A.F. are Investigators of the Howard Hughes Medical Institute. The data presented in this manuscript are tabulated in the main paper and in the supplementary materials.

References and Notes

1. Flegal KM, Graubard BI, Williamson DF, Gail MH. JAMA. 2007; 298:2028. [PubMed: 17986696]
2. Qatanani M, Lazar MA. Genes Dev. 2007; 21:1443. [PubMed: 17575046]
3. Martinez FO, Sica A, Mantovani A, Locati M. Front Biosci. 2008; 13:453. [PubMed: 17981560]
4. Shaul ME, Bennett G, Strissel KJ, Greenberg AS, Obin MS. Diabetes. 2010; 59:1171. [PubMed: 20185806]

5. Weisberg SP, et al. *J Clin Invest*. 2003; 112:1796. [PubMed: 14679176]
6. Lumeng CN, Bodzin JL, Saltiel AR. *J Clin Invest*. 2007; 117:175. [PubMed: 17200717]
7. Lumeng CN, DelProposto JB, Westcott DJ, Saltiel AR. *Diabetes*. 2008; 57:3239. [PubMed: 18829989]
8. Patsouris D, et al. *Cell Metab*. 2008; 8:301. [PubMed: 18840360]
9. Kang K, et al. *Cell Metab*. 2008; 7:485. [PubMed: 18522830]
10. Odegaard JI, et al. *Cell Metab*. 2008; 7:496. [PubMed: 18522831]
11. Odegaard JI, et al. *Nature*. 2007; 447:1116. [PubMed: 17515919]
12. Sabio G, Davis RJ. *Trends Biochem Sci*. 2010; 35:490. [PubMed: 20452774]
13. Solinas G, et al. *Cell Metab*. 2007; 6:386. [PubMed: 17983584]
14. Sabio G, et al. *Science*. 2008; 322:1539. [PubMed: 19056984]
15. Vallerie SN, Furuhashi M, Fucho R, Hotamisligil GS. *PLoS One*. 2008; 3:e3151. [PubMed: 18773087]
16. Hirosumi J, et al. *Nature*. 2002; 420:333. [PubMed: 12447443]
17. Davis RJ. *Cell*. 2000; 103:239. [PubMed: 11057897]
18. Mantovani A, et al. *Trends Immunol*. 2004; 25:677. [PubMed: 15530839]
19. Kitade H, et al. *Diabetes*. 2012; 61:1680. [PubMed: 22474027]
20. Wang J, Beekhuizen H, van Furth R. *Clin Exp Immunol*. 1994; 95:263. [PubMed: 7508346]
21. Yang DD, et al. *Immunity*. 1998; 9:575. [PubMed: 9806643]
22. Dong C, et al. *Science*. 1998; 282:2092. [PubMed: 9851932]
23. Dong C, et al. *Nature*. 2000; 405:91. [PubMed: 10811224]
24. Das M, et al. *Cell*. 2009; 136:249. [PubMed: 19167327]

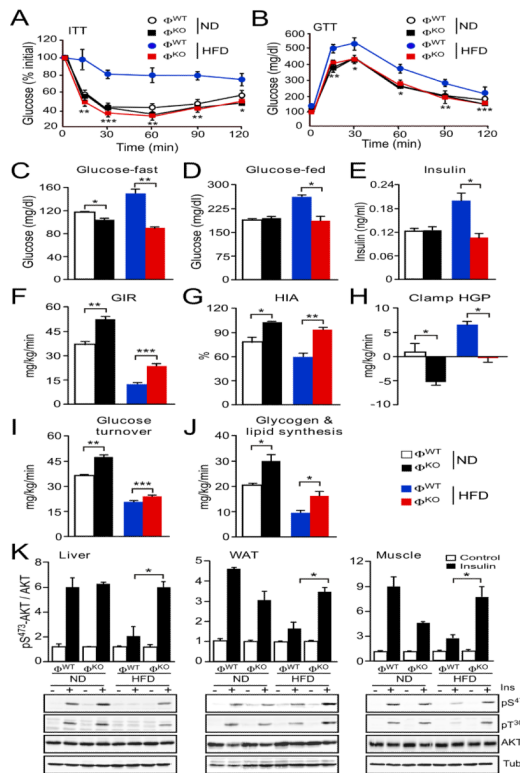


Fig. 1. Macrophage JNK promotes the establishment of obesity-induced insulin resistance. (A) Insulin tolerance tests (ITT) were performed on chow diet and HFD-fed ^{WT} and ^{KO} mice (4 wk.) by intraperitoneal (i.p.) injection of insulin (0.75 U/kg) and measurement of blood glucose concentration (mean \pm S.E.M.; $n = 7 \sim 10$ mice). (B) Glucose tolerance tests (GTT) were performed by i.p. injection of glucose (1 g/kg) and measurement of blood glucose concentration (mean \pm S.E.M.; $n = 7 \sim 10$ mice). (C–E) The blood concentration of glucose and insulin in overnight fasted mice and the blood glucose concentration in fed mice were measured (mean \pm S.E.M.; $n = 10$ mice). (F–J) Insulin sensitivity was measured using a hyperinsulinemic-euglycemic clamp in conscious mice. The steady-state glucose infusion rate (GIR), hepatic insulin action (HIA), clamp hepatic glucose production (HGP), whole body glucose turnover, and whole body glycogen plus lipid synthesis are presented (mean \pm S.E.M.; $n = 8 \sim 10$ mice). (K) Chow-fed (ND) and HFD-fed mice (4 wk.) were fasted overnight and then treated by i.p. injection with 1 U/kg insulin (15 min). Multiplexed ELISA was used to detect AKT and activated (pSer⁴⁷³) AKT in the liver, epididymal adipose tissue (WAT), and gastrocnemius muscle (mean \pm S.E.M.; $n = 3 \sim 5$ mice). Representative tissue samples were also examined by immunoblot analysis by probing with antibodies to phospho-AKT, AKT, and Tubulin (Tub.). Data (A–E) are representative of three experiments. Data were pooled from (F–J) eight to ten and (K) three to five experiments. * $P < 0.05$, ** $P < 0.01$, *** $P < 0.001$ as determined by Student's t test (A,B) or ANOVA with Bonferroni's posttest correction for multiple comparisons (C–K).

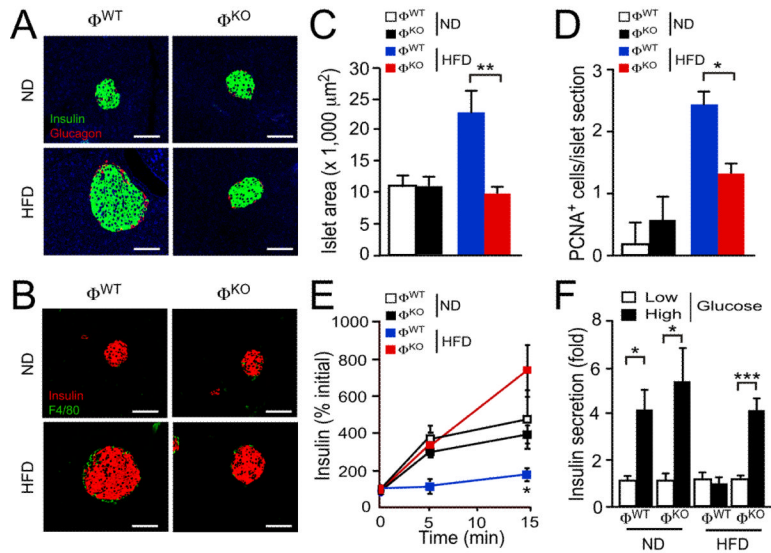
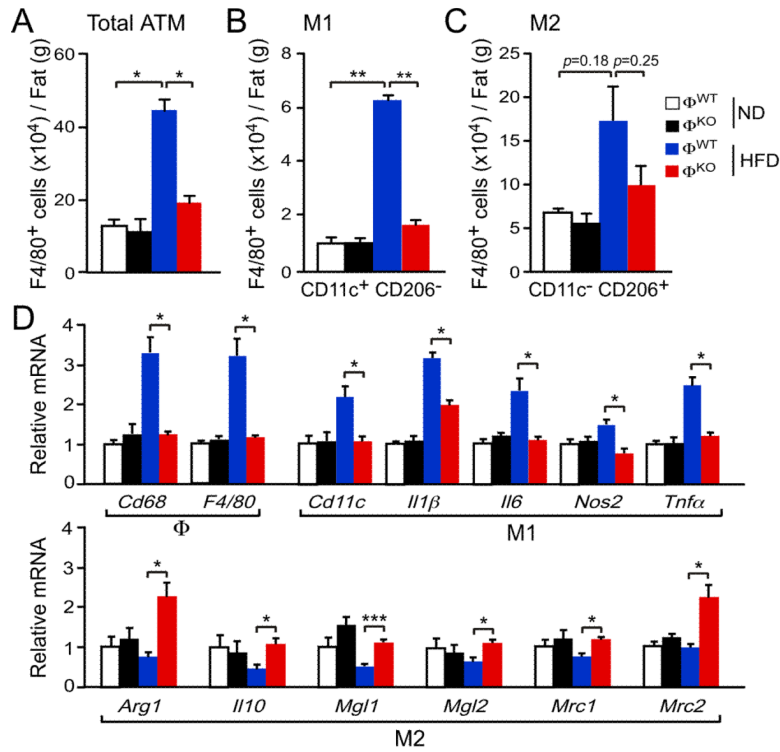
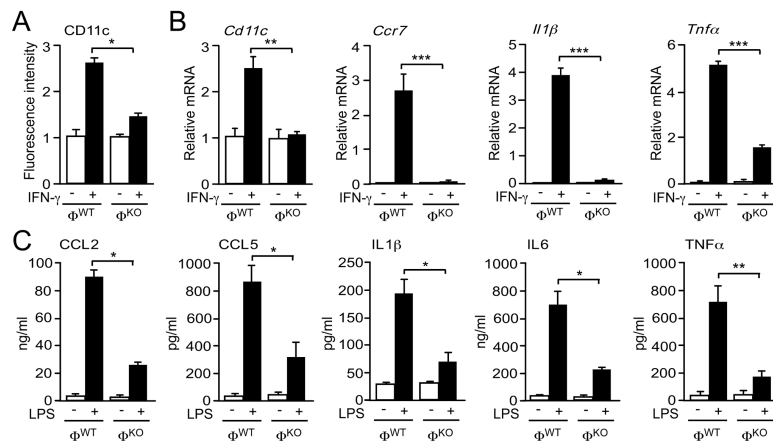


Fig. 2. Macrophage JNK promotes pancreatic islet dysfunction. **(A,B)** The morphology of pancreatic islets was examined using chow-fed (ND) and HFD-fed mice (4 wk.) fasted overnight. Sections were stained with antibodies to insulin, glucagon, or F4/80. DNA was stained with DAPI (blue). Scale bar, 75 μm . No significant differences between ϕ^{WT} and ϕ^{KO} islet infiltration by F4/80⁺ macrophages were detected (fig. S19). **(C)** The islet area per section is presented (mean \pm S.E.M.; $n = 7 \sim 10$ mice). **(D)** The number of cells per islet that stained with an antibody to the proliferation marker PCNA is presented (mean \pm S.E.M.; $n = 5 \sim 7$ mice). **(E)** Glucose-induced insulin release measurements were performed by i.p. injection of glucose (2 g/kg) and measurement of blood insulin concentration (mean \pm S.E.M.; $n = 8 \sim 10$ mice). **(F)** Glucose-induced insulin secretion *in vitro*. Isolated islets were incubated (1 hr) with low glucose (3.3 mM) or high glucose (16.7 mM). Insulin secretion was measured (mean \pm S.E.M.; $n = 5$ mice). Data (A,B) are representative of (A,B) five to ten, (E) three, and (F) two experiments. Data (C,D) were pooled from five to ten experiments. * $P < 0.05$, ** $P < 0.01$, *** $P < 0.001$ as determined by Student's *t* test (E) or ANOVA with Bonferroni's posttest correction for multiple comparisons (C,D,F).

**Fig. 3.**

JNK promotes M1 polarization of adipose tissue macrophages. (A–C) The stromal vascular fraction (SVF) of epididymal adipose tissue was isolated from chow-fed and HFD-fed (4 wk.) mice and examined by flow cytometry to detect the total number of F4/80⁺ adipose tissue macrophages (ATM), the number of F4/80⁺ CD11c⁺ CD206⁻ (M1 ATM), and the number of F4/80⁺ CD11c⁻ CD206⁺ (M2 ATM) (mean \pm S.E.M.; $n = 5$ mice). (D) Total RNA was isolated from epididymal adipose tissue from chow-fed and HFD-fed Φ^{WT} and Φ^{KO} mice. The relative expression of mRNA associated with M1-polarized macrophages and M2-polarized macrophages was measured by quantitative RT-PCR assays (mean \pm S.E.M.; $n = 8 \sim 10$ mice). Data (A–C) are representative of three experiments. Data (D) were pooled from eight to ten experiments. * $P < 0.05$, ** $P < 0.01$, *** $P < 0.001$ as determined by ANOVA with Bonferroni's posttest correction for multiple comparisons.

**Fig. 4.**

JNK promotes M1 polarization of macrophages *in vitro*. (A) Bone marrow-derived macrophages (BMDM) from ϕ WT and ϕ KO mice were incubated without or with 100 ng/ml IFN- γ (36 hr). F4/80 $^{+}$ cells were stained with an antibody to the M1 marker CD11c and examined by flow cytometry (mean relative fluorescence intensity \pm S.E.M.; $n = 3$). (B) Total RNA was isolated from BMDM incubated (8 hr) with 100 ng/ml IFN- γ . The relative expression of the indicated M1 marker genes was measured by quantitative RT-PCR assays (mean \pm S.E.M.; $n = 5$ mice). (C) Chow-fed ϕ WT and ϕ KO mice were fasted overnight. Blood was collected from the mice 2.5 hr after i.p. injection of LPS (20 mg/kg) or solvent (Control). The blood concentration of CCL2, CCL5, IL1 β , IL6, and TNF α was measured (mean \pm S.E.M.; $n = 10$ mice). Data are representative of (A) three and (C) two experiments. Data (B) were pooled from five experiments. * $P < 0.05$, ** $P < 0.01$, *** $P < 0.001$ as determined by ANOVA with Bonferroni's posttest correction for multiple comparisons.